



Semnan University

Mechanics of Advanced Composite Structures

journal homepage: <http://MACS.journals.semnan.ac.ir>

Free Vibration Analysis of Graphene Reinforced Laminated Composite Plates using Experimental Modal Testing

M. S. Koppanati ^{a*}, M. Naga Rani ^b, K. Krishna Bhaskar ^c

^a Professor, Department of Mechanical Engineering, University College of Engineering Kakinada (A), Kakinada, 533003, India.

^b M.Tech Student in University College of Engineering Kakinada (A) Kakinada, 533003, India.

^c Assistant Professor, Department of Mechanical Engineering, University College of Engineering, JNTUK Kakinada, Kakinada, India.

KEYWORDS

Halpin-Tsai model;
Finite element method;
Stacking sequence;
Experimental modal analysis;
Fast Fourier transform.

ABSTRACT

Graphene has become a significant and handy nanomaterial due to its excellent tensile strength, electrical conductivity, and stiffness, and is the thinnest material. It could be utilized to reinforce the polymer matrix of composites, increasing their strength and stiffness. In this study, the vibration behaviour of carbon fiber graphene-reinforced hybrid polymer plate, graphene-reinforced polymer plate, and carbon fiber-reinforced polymer plate (CFRP), is examined in the context of developing laminated composite plates. The material properties of the graphene-reinforced matrix are estimated using the applicable Halpin-Tsai models. Following that, the orthotropic mechanical properties of a composite carbon fiber and hybrid matrix lamina are evaluated. Plates are modeled using finite element modeling methods while taking into account a specific stacking order and geometric layouts. The impact hammer modal testing method is used to document the plates' reaction to vibration. In order to see the intrinsic frequencies and mode shapes of the plate, the recorded time domain responses are translated to the frequency domain using the Fast Fourier transform (FFT). The ME Scope software is used for post-processing. The modes of vibration response are assessed by applying various boundary conditions. Results indicate that natural frequencies increase with increasing graphene volume fraction. The larger the volume percentage, the higher the plate's frequency for all transverse modes, as seen. By incorporating 1% graphene into the polymer matrix, the first, second, third, and fourth mode forms increase by up to 32.35%, 48.96%, 22.17%, and 30.08%, respectively. Adding graphene to the composite raises the frequency of higher modes relative to the basic mode.

1. Introduction

Polymer matrix composites offer great strength and stiffness while being lightweight, making them a viable choice for Aerospace, Automotive, Medical, and other technical applications. Graphene's high mechanical performance allows it to be utilized to strengthen polymer matrix composites, increasing strength and stiffness.

Carbon fiber reinforced polymers have high strength and stiffness as well as good corrosive resistance which can be extensively used for marine applications as well as aerospace

applications. Graphene is a carbon allotrope, which is 200 times stronger than steel. Nowadays, Graphene nanoplatelets are used as fillers in composite materials which enhances the mechanical properties of the composite structures.

Pre-mixing nanoparticles into the polymer matrix may improve through-thickness or matrix-dominant characteristics. Combining spray coating with vacuum-assisted resin infusion resulted in a process for producing CFRP hybrid composites with the desirable in-plane

* Corresponding author. Tel.: 8008612555
E-mail address: meera.aec@gmail.com

aligned graphene nanoplatelets, according to Yao [1] findings.

The tensile, flexural, and CO₂ gas permeability of the material was assessed. It was demonstrated that under relatively modest GNP loadings (0.2 vol %), both tensile and flexural properties performed better, however, the gas barrier property improved dramatically as GNP loadings increased.

First-order shear deformation plate theory is used to create the theoretical formulation, and thermo-elastic equilibrium equations are solved to get the initial thermal stresses. To assess the effective material properties of each layer of the composite plates reinforced graphene nanoparticles, the Halpin-Tsai micromechanical model is applied. Qaderi [2] concluded that as the Graphene platelets' weight fraction rises; the dimensionless frequency of graphene-reinforced composite plates gets better. Regardless of the Graphene platelet distribution pattern, the dimensional less natural frequency rises when graphene platelets are introduced into an epoxy matrix. Soykok [3] used two distinct ways to theoretically establish the engineering constants of CNT and carbon fiber-reinforced composite laminates. They employed the finite element approach to model and investigate the behaviour of a certain stacking sequence and composite plate design under static loadings. Their findings show a considerable enhancement in plate stiffness due to the presence of nanotubes. Hulun et al. [4] used the element-free Improved Moving Least Squares-Ritz approach to examine the free vibration response of graphene-reinforced composite quadrilateral plates. They came to the conclusion that raising the weight percentage of GPLs can increase the natural frequency of a quadrilateral plate.

Mishra et al. [18] performed the vibration analysis of the composite plates both analytically and numerically. The research was done on the UD fiber GFRP woven fabric composite plates at free-free test conditions. The authors mentioned that the analysis was performed using modern testing methods and analysis was done using computerized software. Results indicate that the natural frequency of the composite plate with the CL condition is very less when compared with the SS condition.

Patel et al. [19] conducted a study on the experimental and numerical analysis of the free vibrations of MWCNTRCP. The authors studied the effects of different percentages of MWCNT on the NFs of FRP by varying the thickness, aspect ratios, and boundary conditions. The manufacturing technique used to fabricate the composite plate was the Manual Hand layup technique. The authors also stated that the elastic properties were determined using experimental

techniques. In this research, an advanced simulation, known as ABAQUS, was used to determine the modal response of the composites and compared them with the experimental ones. Results indicate that there is an increase in the elastic properties and NF's up to 0.3 wt. % of MWCNT and thereafter decreases gradually due to agglomeration of CNT in a polymer matrix.

Prasad et al. [20] research has been carried out on the experimental and numerical study of the vibration analysis of the woven FML plates. The authors stated that they initiated the work using the first-order Reissner-Mindlin theory with the FE formulations for both fibers and metals. The NFs were obtained by performing the experimental analysis using B & K FFT analyzer. Results also include that as the thickness ratio is decreased the NF of the FML increased. It is also declared that the type of boundary condition may affect the NF of the FML plate.

Prasad et al. [21] performed experimental work on the fatigue characteristics of the FML with the effect of the Nano alumina. In this article, the authors stated that the addition of Nanofillers to the composite material increases the binding strength of the composite. The experimental test such as the low cycle fatigue test indicated that as the percentage of the Nanofillers are increasing so as the fatigue characteristics of the composite also increase. Maximum UTS of about 70% was found at 94% of FBL.

Sahu et al. [22] conducted numerical prediction and experimental validation of free vibration responses of the hybrid composite curved panel structure. The authors used a mathematical formulation with 5 modal responses by considering different parameters. Results indicate that the experimental data is correlated with the ANSYS FE data through a static structural module. Also, it indicated that the number of layers and type of fiber affect the frequency due to the stiffness variation.

Sahu. P et al. [23] performed a generic computer code generated via the higher-order mathematical model to calculate the variation in modal responses with temperature increments. The numerical frequency values are compared to the experimental results and the numerical results from other publications.

Using the variation approach [24], the weak form of the governing equation is established by constructing a higher-order kinematic model that takes into account the effect of single and double curvatures, respectively on the shell panel.

Mehar et al. [25] conducted experimental verification on the thermo-mechanical transient flexure on the GCKRHCC shell panels. To perform the numerical research, HOKM is prepared considering the effect of the curvature of the shell panel. The transient vibrations are found using

the governing equations derived from MATLAB and computed through FEM. The validation of the numerical results is then compared with the experimental results.

In this journal [26] thermal free vibration behavior of the nanotube-reinforced SMA bonded composite structural model has been formulated mathematically using the HSDT kind of displacement theory including the nonlinearity due to the embedded functional material. A mathematical model for the thermal free vibration behavior of nanotube-reinforced SMA bonded composite structures has been formulated using the displacement theory including nonlinearity caused by embedded functional materials [27].

The novelty of this [28] work lies in developing a finite component model integrated with the HDMR tool, for a laminated plate with curving fiber, and incorporation of PNN into the model for sensitivity and random analysis, severally. The finite component code developed in MATLAB surroundings is valid completely with the sooner printed literature.

Sharma et al. [29] conducted a stochastic RBFN test and found three completely different fiber distribution patterns and a spread of boundary conditions. For the thermal buckling analysis, uncertainty within the material properties and thermal parameters is taken into consideration. The variance-based world sensitivity analysis is employed to estimate the contribution of every input parameter. In [30] authors performed the aeroelastic analysis of composite laminates with different fiber spacings.

In [31], Sharma et al. performed static and free vibration analysis of LCP with delamination and found that the delamination is an associated degree of inevitable development in composite structures encountered typically in world operative conditions. The presence of delamination among the structure might considerably affect the dynamic response thanks to the reduction of stiffness of the structure.

For aeroelastic analysis, the metal model is as well as a master's degree. Varied constant studies area units were performed to seek out the foremost essential location of the delamination that severely affects vibration and flutter characteristics [32-34]. The results showed that the delamination close to the vanguard that faces free stream wind is found to be the foremost essential for the dynamic aeroelastic failure of structures [35].

In [36] two kinds of sandwich plate sandwiches with FGM face sheets and uniform core and sandwiches with uniform face sheets and FGM core are thought of for gratis vibration analysis with nonlinear temperature variation

over the thickness direction. The higher-order layer-wise theory is adopted with an associate in nursing eight-noded rectangular component to make a finite component model for gratis vibration analysis.

In this study, the vibration behavior of carbon fiber graphene-reinforced hybrid polymer plate, graphene-reinforced polymer plate, and carbon fiber reinforced polymer plate (CFRP), are examined in the context of developing laminated composite plates. The material properties of the graphene-reinforced matrix are estimated using the applicable Halpin-Tsai models. Following that, the orthotropic elastic constants of a composite carbon fiber and hybrid matrix lamina are evaluated. Plates are modeled using finite element modeling methods (ANSYS APDL Software) while taking into account specific stacking order and geometric layouts. The impact hammer modal testing method is used to document the plates' reaction to vibration.

2. Materials and Modeling

2.1. Materials and Specimen Geometries

Materials used for the carbon fiber reinforced plate (CFRP) are carbon fiber as reinforcement, and polyester resin as the matrix. For Graphene reinforced polymer plate (GRP), Graphene Nanoplatelets as reinforcement and Polyester resin as the matrix. For carbon fiber graphene reinforced hybrid plate, Carbon, Graphene nanoplatelets as reinforcement, and Polyester resin as the matrix. The Quasi-elastic lamination Sequence of both eight-layered unidirectional fibers of the CFRP plate and Hybrid plate is [0/45/-45/90/90/-45/45/0]. The GRP plate is a single-layered plate with a 3 mm thickness.

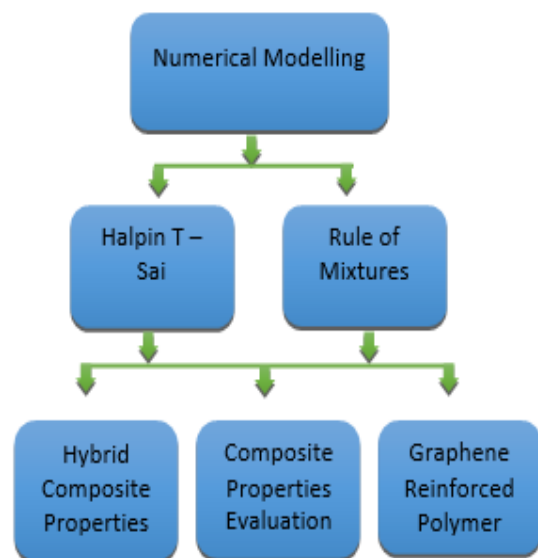


Fig. 1. Numerical modeling of Composite plates

The ASTM D7264 standard specifies that plates are modeled and fabricated using a hand layup process with dimensions of W, L, and T (W, L, and T) greater than or equal to 10 T.

Table 1. Dimensions of plate

| Dimension | CFRP Plate | GRP Plate | Hybrid Plate |
|---------------|------------|-----------|--------------|
| Length (L) | 250mm | 245mm | 250mm |
| Width (W) | 250mm | 245mm | 250mm |
| Thickness (T) | 3mm | 3mm | 3mm |

Table 2 below provides the measurements of all three plates.

2.2. Halpin-Tsai Model

According to the Halpin-Tsai model, Young's modulus of the graphene and polymer matrix may be estimated using the following equation [8].

$$E_{m-gpl} = \frac{1}{5}E_L + \frac{4}{5}E_T \tag{1}$$

where

$$E_L = \frac{1 + \xi_L \eta_L V_{gpl}}{1 - \eta_L V_{gpl}} E_m \tag{2}$$

$$E_T = \frac{1 + \xi_T \eta_T V_{gpl}}{1 - \eta_T V_{gpl}} E_m \tag{3}$$

$$\eta_L = \frac{\frac{E_{gpl} - 1}{E_m}}{\frac{E_{gpl} - 1}{E_m} + \xi_L}, \eta_T = \frac{\frac{E_{gpl} - 1}{E_m}}{\frac{E_{gpl} - 1}{E_m} + \xi_T} \tag{3}$$

$$\xi_L = 2 \frac{L_{gpl}}{T_{gpl}}, \xi_T = 2 \frac{W_{gpl}}{T_{gpl}} \tag{4}$$

where V_{gpl} and T_{gpl} represent the graphene volume fraction and thickness of graphene, respectively. Furthermore, E_m is the Polymer matrix's Young's modulus, whereas $\xi_L, \xi_T, \eta_L,$ and η_T are Halpin-Tsai parameters that depend on the shape of the reinforcement. Assuming that Poisson's ratio ν_m , Shear modulus G_{m-gpl} , Density ρ_{m-gpl} are

$$\nu_{m-gpl} = \nu_m \tag{5}$$

$$G_{m-gpl} = \frac{E_{m-gpl}}{2(\nu_{m-gpl} + 1)} \tag{6}$$

$$\rho_{m-gpl} = V_{gpl} \rho_{gpl} + V_m \rho_m \tag{7}$$

When considering a unidirectional lamina, the standard rule of a mixture can be used to obtain its modulus of elasticity in the longitudinal direction, E_1 , and Poisson's ratio, ν_{12} of Hybrid plate,

$$E_1 = E_{f1} V_f + E_{m-gpl} V_{m-gpl} \tag{8}$$

$$\nu_{12} = \nu_f V_f + \nu_{m-gpl} V_{m-gpl} \tag{9}$$

where $E_{f1}, V_f, \nu_f,$ and V_{m-gpl} are longitudinal Young's modulus and volume fraction of fiber, Poisson's ratio of fiber and volume fraction of the hybrid plate, severally.

The material properties of Plates by adding 1% by weight ($V_{gr} = 0.005$) of Graphene Nanoplatelets into the matrix are listed in Table 3. Values in Table 3 are obtained by equations 1 - 9.

Table 2. Properties of components of the composite material

| | Carbon fiber[5] | | Polyester resin[6] | | Graphene[7] |
|-------------------------------|-----------------|-------------------------------|--------------------|-----------------------------------|-------------|
| E_{f1} (GPa) | 230 | E_m (GPa) | 3 | E_{gpl} (GPa) | 735 |
| E_{f2} (GPa) | 15.4 | ν_m | 0.316 | W_{gpl} (nm) | 10.02 |
| ν_{f23} | 0.46 | G_m (GPa) | 1.139 | L_{gpl} (nm) | 9.97 |
| ν_{f12} | 0.29 | ρ_m (Kg/m ³) | 1200 | ρ_{gpl} (Kg/m ³) | 2260 |
| G_{f12} (GPa) | 10 | | | | |
| G_{f23} (GPa) | 5.28 | | | | |
| ρ_f (Kg/m ³) | 1800 | | | | |

Table 3. Material properties of Composite plates

| Material Property | CFRP Plate | GRP plate | Hybrid Plate |
|-------------------------------|------------|-----------|--------------|
| E_{11} (GPa) | 139.20 | 3.197 | 139.28 |
| E_{22} (GPa) | 7.799 | 3.199 | 10.52 |
| E_{33} (GPa) | 7.799 | 3.199 | 10.52 |
| ν_{12} | 0.3 | 0.315 | 0.3 |
| ν_{23} | 0.397 | 0.315 | 0.397 |
| ν_{13} | 0.3 | 0.315 | 0.3 |
| G_{12} (GPa) | 4.924 | 1.215 | 6.51 |
| G_{23} (GPa) | 3.493 | 1.216 | 3.65 |
| G_{13} (GPa) | 4.924 | 1.215 | 6.51 |
| ρ_c (Kg/m ³) | 1560 | 1205 | 1562 |

2.3. Finite Element Modeling

In ANSYS 19.2 Mechanical APDL Software, the plates are modeled as a plane region, and eight-noded quadrilateral shell elements are used for meshing (SHELL281). For evaluating thin to moderately thick shell structures, use the SHELL281 element. The element has eight nodes, each of which has six degrees of freedom: translations along the x, y, and z axes, as well as rotations about these axes. The first-order shear deformation theory (FSDT), which assumes that the transverse shear strain is constant throughout the thickness of the shell, governs the accuracy of modeling composite shells employing these elements [9].

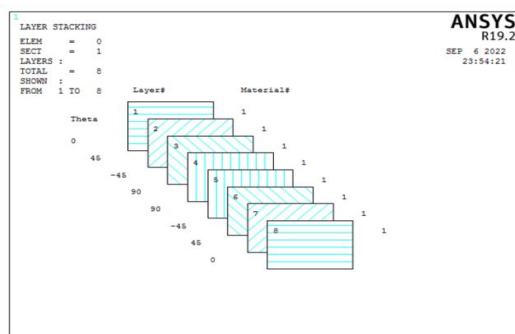


Fig. 2. 8 Layered composite laminate plate in ANSYS

3. Experimentation

Three plates with two end conditions, such as Clamped - Free - Clamped - Free (CFCF) and Simply Supported - Free - Simply Supported - Free (SFSF), are subjected to experimental modal analysis (EMA) to determine the vibration behavior and dynamic features. The experimental setup for modal analysis illustrates how a free vibration test performs a modal analysis. By converting the vibration motion into electrical signals, an accelerometer may measure the sample response and vibration levels at various locations on a structure. Using beeswax, (commercial) the accelerometer was attached to the sample.

An exciting shock is delivered using an impact hammer with a quartz tip to establish the initial input frequency and magnitude for the modal setup. To obtain the sample I/O data, a unit with eight input channels was used. To take measurements, two input channels are chosen, the first of which is coupled to an accelerometer, and the second of which is attached to an impact hammer. To ascertain the dynamic characteristics and modal characteristics, including natural frequencies and mode shapes, a data acquisition system (DAQ) is employed. Using the SAMURAI software tool, these data were retrieved from frequency response function curves (FRF).

The ME'Scope Software is used for post-processing. The natural frequencies will be extracted from the FRFs obtained from the testing throughout this module, and they will be assigned to the ME Scope structure along with the FRFs in order to produce the animation of Mode shapes.

The following apparatus will be used to perform the experiment:

1. Impact Hammer.
2. Uni-axial Accelerometer.
3. Multi-channel Vibration Analyzer (At least two-channel).
4. A PC or a Laptop loaded with software for modal analysis.
5. Test-specimen.
6. ME'Scope Software
7. SAMURAI Software

The experimental setup with various boundary conditions was shown in Figures 3 to 9.



Fig. 3. Experimental Setup



Fig. 4. CFRP square plate with CFCF Boundary condition

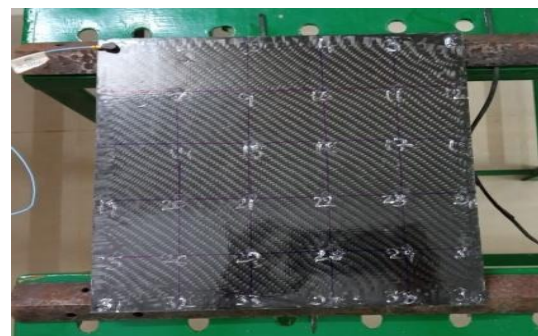


Fig. 5. Hybrid square plate with SFSF Boundary condition

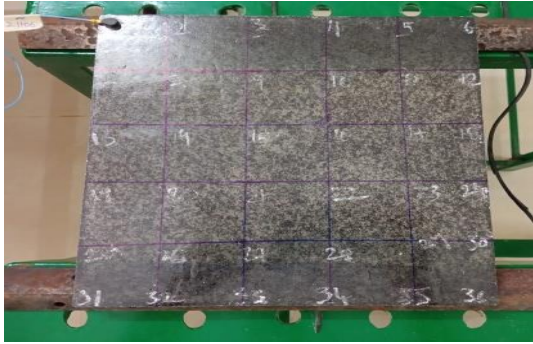


Fig. 6. GRP square plate with SFSF boundary condition

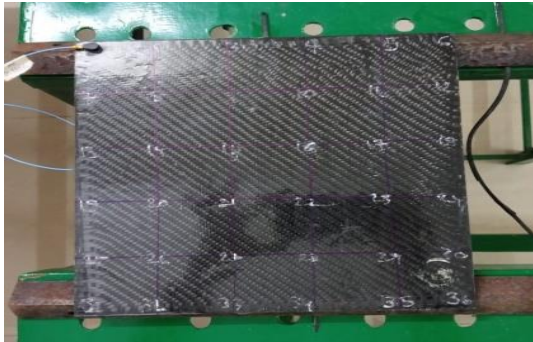


Fig. 7. CFRP square Plate with SFSF Boundary condition

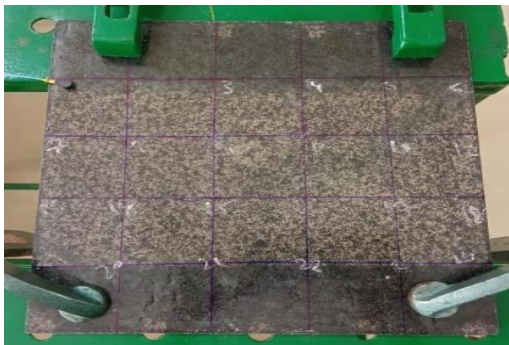


Fig. 8. GRP square plate with CFCF Boundary condition



Fig. 9. Hybrid square plate with CFCF Boundary condition

4. Results and Discussions

The results for Natural frequencies and mode shapes of all three plates are discussed in this section. The ANSYS results for natural frequencies and mode shapes are evaluated and compared with the experiment results.

4.1 Carbon Fiber Reinforced Plate (CFRP)

Tables 4 and 5 show the natural frequencies of carbon fiber reinforced plates with SFSF and CFCF boundary conditions compared with ANSYS and experimentation.

Table 4. Natural frequencies of CFRP square plate with SFSF boundary condition

| Mode Number | EMA (Hz) | ANSYS (Hz) | Percentage Difference (%) |
|-------------|----------|------------|---------------------------|
| 1 | 87.5 | 97.4 | 10.16 |
| 2 | 125 | 134 | 6.71 |
| 3 | 241 | 247 | 2.42 |

Table 5. Natural frequencies of CFRP square plate with CFCF boundary condition

| Mode Number | EMA (Hz) | ANSYS (Hz) | Percentage Difference (%) |
|-------------|----------|------------|---------------------------|
| 1 | 322 | 332 | 3.01 |
| 2 | 366 | 365 | 0.27 |
| 3 | 497 | 494 | 0.60 |

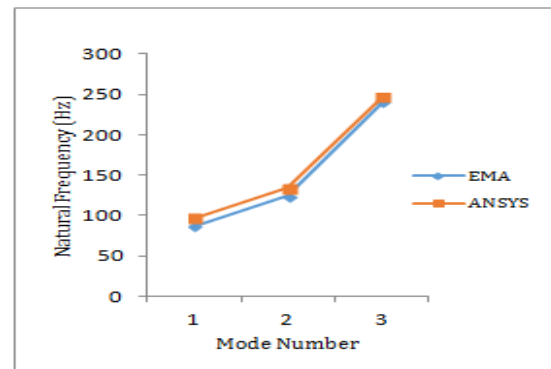


Fig. 10. Natural frequencies of CFRP square plate with SFSF boundary condition

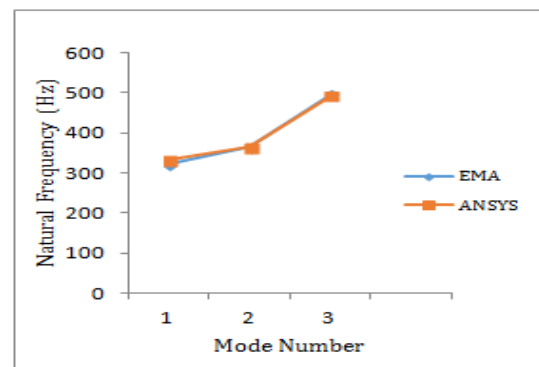


Fig. 11. Natural frequencies of CFRP square plate with CFCF boundary condition

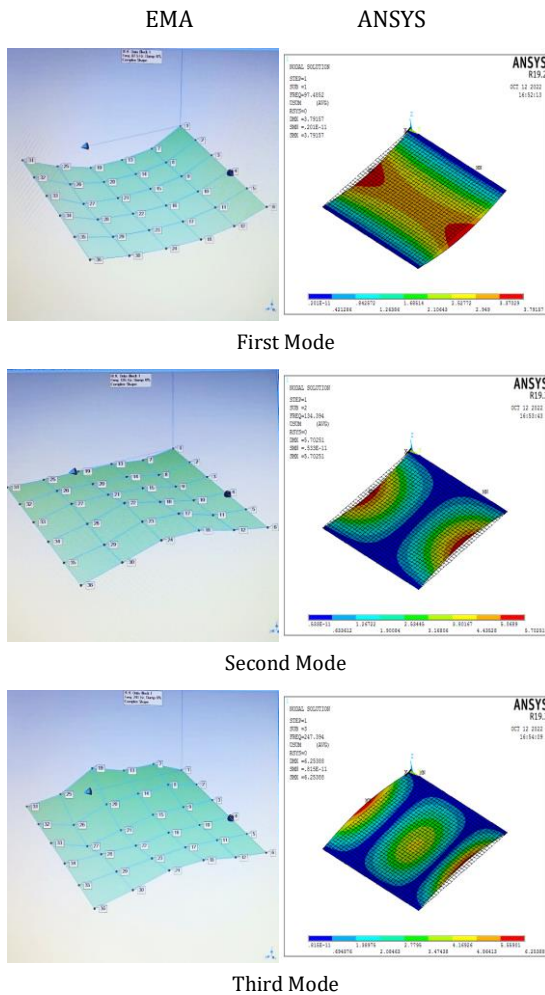


Fig. 12. Variation of mode shapes for SFSF CFRP square plate with experimental modal testing and ANSYS

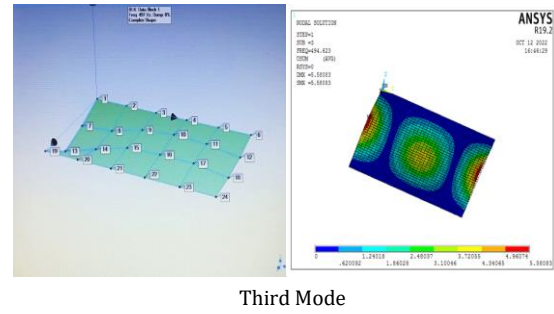
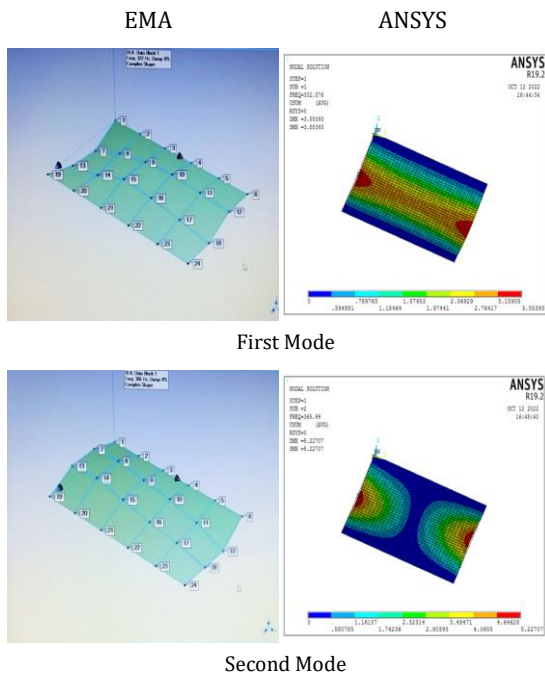


Fig. 13. Variation of mode shapes for CFCF CFRP square plate with experimental modal testing and ANSYS

As observed from the above values of natural frequencies for both SFSF and CFCF conditions, CFCF has higher natural frequencies than SFSF, as the stiffness of clamped condition is more than the supported condition.

The results obtained from experimental modal testing agreed well with ANSYS results. Visual representation of mode shapes was given in Figures 12 and 13.

4.2. Graphene Reinforced Polymer Plate (GRP)

Graphene nanoplatelets are uniformly and randomly oriented all over the plate with a single layer thickness of 3mm.

Tables 6 and 7 show the natural frequencies of the graphene-reinforced plate with SFSF and CFCF boundary conditions compared with ANSYS and experimentation.

Table 6. Natural frequencies of GRP square plate with SFSF boundary condition

| Mode Number | EMA (Hz) | ANSYS (Hz) | Percentage Difference (%) |
|-------------|----------|------------|---------------------------|
| 1 | 43.8 | 37.8 | 13.69 |
| 2 | 75 | 62.6 | 16.53 |
| 3 | 134 | 143 | 5.59 |

Table 7. Natural frequencies of GRP square plate with CFCF boundary condition

| Mode Number | EMA (Hz) | ANSYS (Hz) | Percentage Difference (%) |
|-------------|----------|------------|---------------------------|
| 1 | 119 | 116 | 2.52 |
| 2 | 156 | 137 | 12.17 |
| 3 | 238 | 226 | 5.04 |

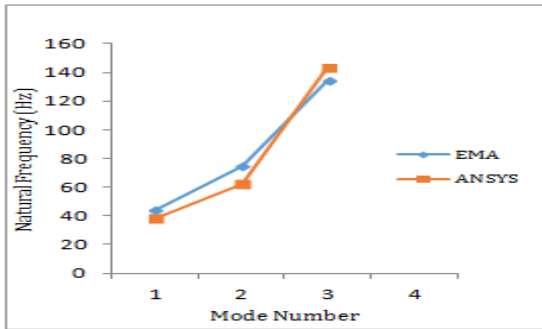


Fig. 14. Natural frequencies of GRP square plate with SFSF boundary condition

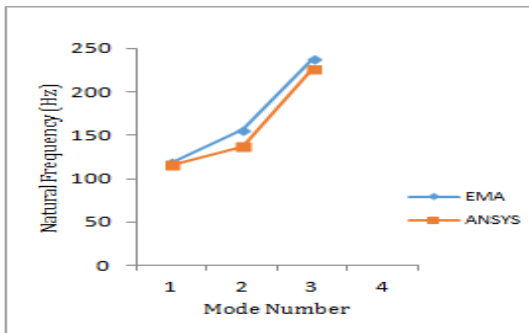
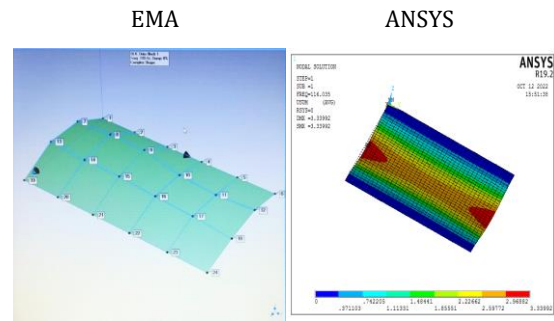
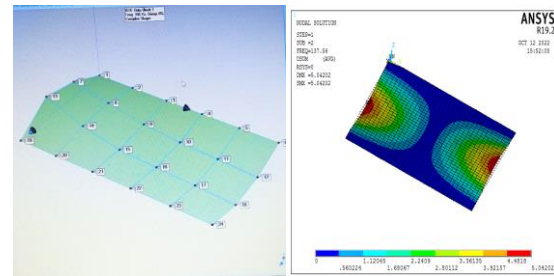


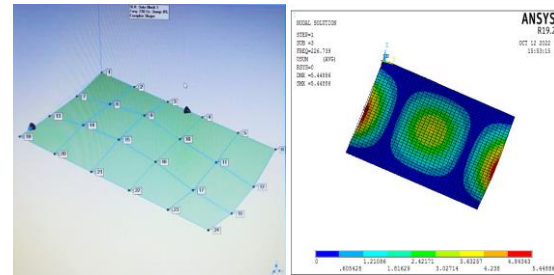
Fig. 15. Natural frequencies of GRP square plate with CFCF boundary condition



First Mode



Second Mode



Third Mode

Fig. 17. Variation of mode shapes for CFCF GRP square plate with Experimental modal testing and ANSYS

As observed from the above values of natural frequencies for both SFSF and CFCF conditions, CFCF has high natural frequencies than SFSF. As the stiffness of clamped condition is more than the supported condition.

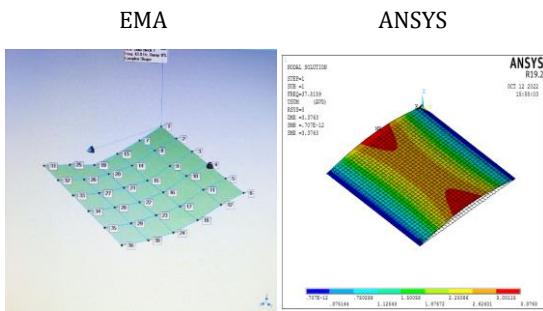
The results obtained from experimental modal testing agreed well with ANSYS results. Visual representation of mode shapes was given in Figures 16 and 17.

4.3. Carbon Fiber – Graphene – Reinforced Hybrid Plate

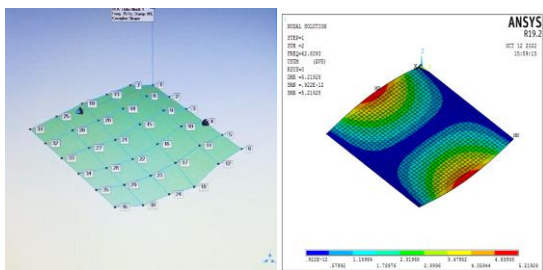
Tables 8 and 9 show the natural frequencies of the graphene-reinforced plate with SFSF and CFCF boundary conditions compared with ANSYS and experimentation.

Table 8. Natural frequencies of Hybrid square plate with SFSF boundary condition

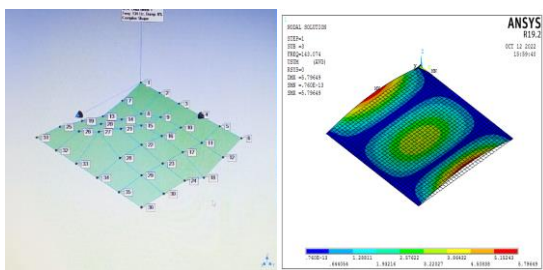
| Mode Number | EMA (Hz) | ANSYS (Hz) | Percentage Difference (%) |
|-------------|----------|------------|---------------------------|
| 1 | 90.6 | 97.4 | 6.98 |
| 2 | 128 | 134.4 | 4.76 |
| 3 | 244 | 247 | 1.21 |



First Mode



Second Mode



Third Mode

Fig. 16. Variation of mode shapes for SFSF GRP square plate with experimental modal testing and ANSYS

Table 9. Natural frequencies of Hybrid square plate with CFCF boundary condition

| Mode Number | EMA (Hz) | ANSYS (Hz) | Percentage Difference (%) |
|-------------|----------|------------|---------------------------|
| 1 | 328 | 333 | 1.50 |
| 2 | 369 | 366 | 0.81 |
| 3 | 475 | 497 | 4.42 |

As observed from the above values of natural frequencies for both SFSF and CFCF conditions, CFCF has high natural frequencies than SFSF, as the stiffness of clamped condition is more than supported condition.

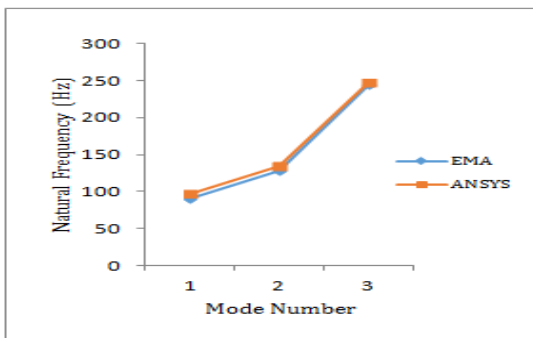
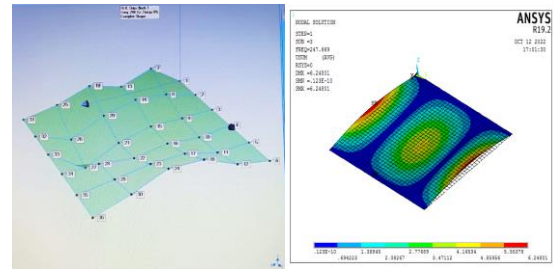


Fig. 18. Natural frequencies of Hybrid square plate with SFSF boundary condition

The results obtained from the Experimental modal testing very well agreed with ANSYS results. Visual representation of mode shapes was given in Figures 19 and 20.



Third Mode

Fig. 19. Variation of mode shapes for SFSF hybrid square plate with experimental modal testing and ANSYS

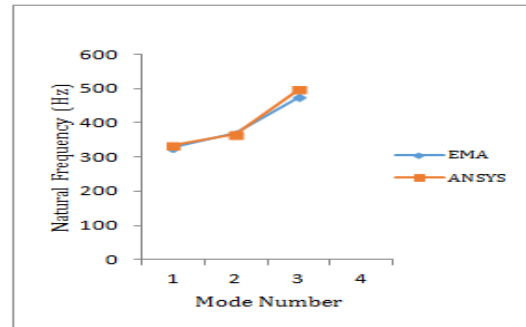
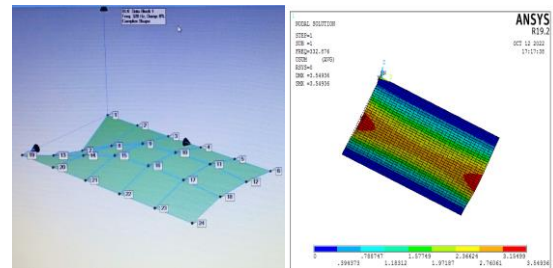


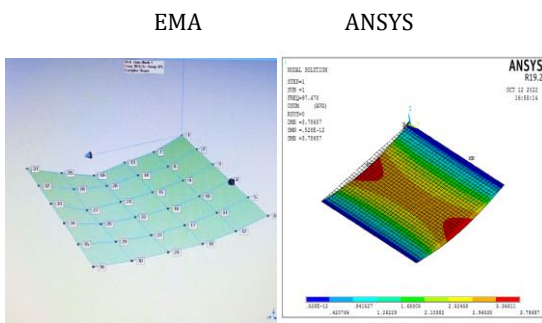
Fig. 20. Natural frequencies of Hybrid square plate with CFCF boundary condition

EMA

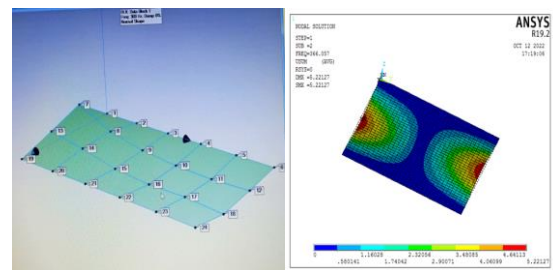
ANSYS



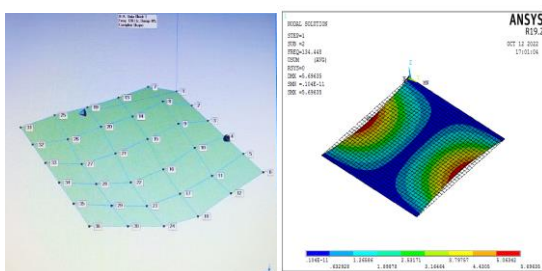
First Mode



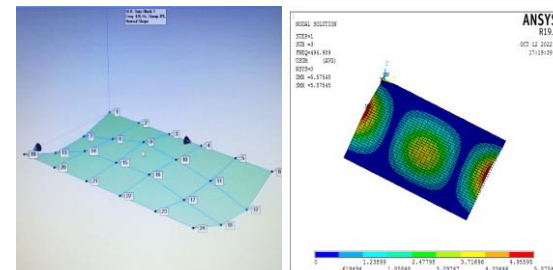
First Mode



Second Mode



Second Mode



Third Mode

Fig. 21. Variation of mode shapes for CFCF hybrid square plate with experimental modal testing and ANSYS

Table 10. Material properties of carbon fiber graphene reinforced hybrid composite plate

| V_{gpl} | E_{11} (GPa) | E_{22} (GPa) | ν_{12} | ν_{23} | G_{12} (GPa) | G_{23} (GPa) | ρ_c (Kg/m ³) |
|-----------|----------------|----------------|------------|------------|----------------|----------------|-------------------------------|
| 0 | 139.20 | 7.799 | 0.30 | 0.397 | 4.924 | 3.493 | 1560 |
| 0.1 | 145.47 | 16.673 | 0.30 | 0.397 | 10.589 | 7.466 | 1602 |
| 0.2 | 152.95 | 23.073 | 0.30 | 0.397 | 14.559 | 11.124 | 1645 |
| 0.3 | 162.00 | 30.305 | 0.30 | 0.397 | 19.010 | 15.445 | 1687 |
| 0.4 | 173.20 | 39.064 | 0.30 | 0.397 | 24.388 | 20.752 | 1730 |
| 0.5 | 187.42 | 50.094 | 0.30 | 0.397 | 31.154 | 27.473 | 1772 |

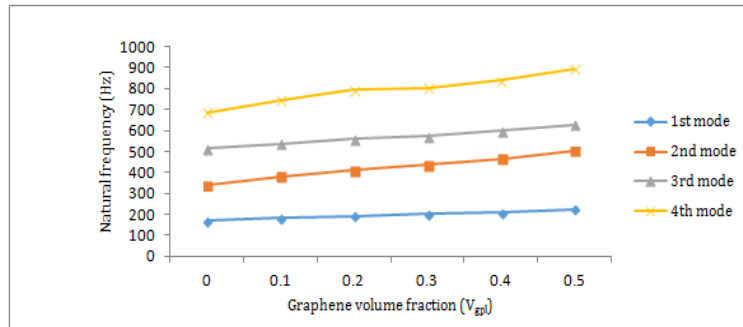


Fig. 22. Effect of Graphene volume fraction on natural frequencies with corresponding mode shapes for all edges simply-supported (SSSS) plate boundary condition

From the results, one can clearly observe that the hybrid plate has higher natural frequencies when compared to the CFRP plate and

GRP plate and the lower Natural frequencies were observed at the GRP plate. This indicates that by adding Graphene nanoplatelets into polymer composite plates, the natural frequencies of plates get increased which implies stiffness of the plate is also increased, and further dynamic characteristics of the plate get enhanced.

4.4. Effect of Graphene Volume Fraction on Carbon Fiber – Graphene – Reinforced Hybrid Plate Assuming SSSS Boundary Condition

The graphene volume fraction is evaluated to find the influence of graphene inclusion on the vibration response of a carbon fiber-graphene-reinforced hybrid plate under SSSS boundary conditions on ANSYS.

To carry out the method, five distinct situations are considered: $V_{gpl} = 0.1, 0.2, 0.3, 0.4,$ and 0.5 . The influence of graphene volume percentage on the first, second, third, and fourth mode forms of transverse vibrations are shown in Fig. 22. The larger the volume percentage, the higher the plate’s frequency for all transverse modes, as seen. By incorporating 50% graphene into the polymer matrix, the first, second, third, and fourth mode forms increase by up to 32.35%, 48.96%, 22.17%, and 30.08%, respectively.

Table 11. Effect of Graphene volume fraction on natural frequencies with corresponding mode shapes for SSSS boundary condition

| V_{gpl} | Mode number | | | |
|-----------|-------------|-----|-----|-----|
| | 1 | 2 | 3 | 4 |
| 0 | 170 | 337 | 514 | 688 |
| 0.1 | 182 | 379 | 537 | 746 |
| 0.2 | 193 | 409 | 559 | 795 |
| 0.3 | 201 | 434 | 575 | 805 |
| 0.4 | 212 | 465 | 599 | 839 |
| 0.5 | 225 | 502 | 628 | 895 |

Unlike traditional experiments that use resin to bind two layers together, combined properties of resin and fiber were imparted to a single layer in order to account for resin's effect, followed by the other layers modeled the same way and simulations were performed. If the boundary conditions were not aligned properly with the support structure, it may cause not detect the natural frequencies and have lower bound values.

5. Conclusions

Laminated composite hybrid plates’ free vibration behavior has been examined in order to find out natural frequencies and mode shapes for various end conditions. An in-depth analysis is done on the impact of graphene volume fraction on the dynamic properties of the hybrid plate reinforced with carbon fiber and graphene.

- 1) The results obtained by experimental modal testing and ANSYS simulation are matching very closely.

- 2) Among the three composite plates, it is observed that the highest natural frequency is obtained for the carbon fiber Graphene hybrid composite plate for both CFCF and SFSF boundary conditions.
- 3) The variation of natural frequency among Graphene hybrid composite plate and CFRP plate close to one another. It indicates that the effect of graphene inclusions on natural frequency is not so significant.
- 4) Graphene incorporation improves the orthotropic mechanical characteristics of polymer composite plates.
- 5) While the order of the modes is affected by the addition of graphene, the sequence of the modes is unaffected.
- 6) By incorporating more graphene into the matrix, the composite plate's natural frequencies are increasing.
- 7) Adding graphene to the composite raises the frequency of higher modes relative to the basic mode.

Acknowledgments

The Authors are thankful to the University College of Engineering (A) Kakinada for providing space and utilizing software and hardware facilities for this research work.

Conflicts of Interest

The author confirms that there are no conflicts of interest with the publication of this article.

References

- [1] Yao, X., Raine, T.P. and Liu, M., 2021. Effect of graphene nanoplatelets on the mechanical and gas barrier properties of woven carbon fiber/epoxy composites. *J Mater Sci* 56, pp.19538–19551.
- [2] Qaderi, S., Ebrahimi, F. and Mahesh, V., 2019. Free Vibration Analysis of Graphene Platelets-Reinforced Composites Plates in Thermal Environment Based on Higher-Order Shear Deformation Plate Theory. *Int. J. Aeronaut. Space Sci.* 20, pp.902–912.
- [3] Tas, H. and Soykok, I.F., 2019. Effects of Carbon Nanotube Inclusion into the Carbon Fiber Reinforced Laminated Composites on Flexural Stiffness: A Numerical and Theoretical Study. *Compos. Part B Eng.* 159, pp.44–52.
- [4] Guo, H.; Cao, S.; Yang, T. and Chen, Y., 2018. Vibration of laminated composite quadrilateral plates reinforced with graphene nanoplatelets using the element-free IMLS-Ritz method. *Int. J. Mech. Sci.* 142, pp.610–621.
- [5] Kara, Y. and Akbulut, H., 2017. Mechanical behavior of helical springs made of carbon nanotube additive epoxy composite reinforced with carbon fiber. *Journal of the faculty of engineering and architecture of gazi university*, 32, pp.417–427.
- [6] Rafiee, M.; Nitzsche, F.; Laliberte, J.; Thibault, J. and Labrosse, M.R., 2019. Simultaneous Reinforcement of Matrix and Fibers for Enhancement of Mechanical Properties of Graphene-Modified Laminated Composites. *Polymer Composites* 40, pp.1732–1745.
- [7] Georgantzinos SK., Giannopoulos GI. and Markolefas SI., 2020. Vibration Analysis of Carbon Fiber-Graphene-Reinforced Hybrid Polymer Composites Using Finite Element Techniques. *Materials*, 13(19), 4225.
- [8] Georgantzinos, S.K., Markolefas, S.I., Mavrommatis, S.A. and Stamoulis, K.P., 2020. Finite element modeling of carbon fiber-carbon nanostructure-polymer hybrid composite structures. *MATEC Web Conferences*, 314, 02004.
- [9] https://www.mm.bme.hu/~gyebro/files/ans_help_v182/ans_elem/Hlp_E_SHELL281.html
- [10] Mitao Song., Sritawat Kitipornchai. and Jie Yang., 2017. Free and forced vibrations of functionally graded polymer composite plates reinforced with graphene nanoplatelets. *Composite structures*, 159, pp.579-588.
- [11] Enrique García-Macías., Luis Rodríguez-Tembleque. and Andrés Sáez, 2018. Bending and free vibration analysis of functionally graded graphene vs. carbon nanotube reinforced composite plates, *Composite Structures*, 186, pp. 123-138.
- [12] Pan, H.G., Wu, Y.S., Zhou, J.N., Fu, Y.M., Liang, X. and Zhao, T.Y., 2021. Free Vibration Analysis of a Graphene-Reinforced Porous Composite Plate with Different Boundary Conditions. *Materials*, 14(14):3879.
- [13] Miao Wang, Yong-Gang Xu, Pizhong Qiao and Zhi-Min Li, 2022. Buckling and free vibration analysis of shear deformable graphene-reinforced composite laminated plates, *Composite Structures*, 280, 114854.
- [14] Miao Wang, Yong-Gang Xu, Pizhong Qiao and Zhi-Min Li, 2019. A two-dimensional elasticity model for bending and free vibration analysis of laminated graphene-reinforced composite beams, *Composite Structures*, 211, pp.364-375.
- [15] G. Mittal, V. Dhand, K.Y. Rhee, S.J. Park and W.R. Lee., 2015. A Review on Carbon Nanotubes and Graphene as Fillers in Reinforced Polymer Nanocomposites. *Journal of industrial and engineering chemistry* 21, 11.
- [16] Lee, J.H., Park, S. J. and Choi, J.W., 2019. Electrical Property of Graphene and Its

- Application to Electrochemical Biosensing. *Nanomaterials*, 9, 297.
- [17] Shahrjerdi, A. and Yavari, S. 2018. Free vibration analysis of functionally graded graphene-reinforced nanocomposite beams with temperature-dependent properties. *J Braz. Soc. Mech. Sci. Eng.* 40, 25
- [18] Mishra, Itishree and Sahu, Shishir. 2015. Modal Analysis of Woven Fiber Composite Plates with Different Boundary Conditions. *International Journal of Structural Stability and Dynamics*. 15. 1540001.
- [19] Patel., Asha, Das., Rahul, Sahu. and Shishir Kumar., 2020. Experimental and Numerical Study on Free Vibration of Multiwall Carbon Nanotube Reinforced Composite Plates. *International Journal of Structural Stability and Dynamics*, 20(12), 2050129.
- [20] Prasad, Elluri and Sahu, Shishir. 2018. Vibration Analysis of Woven Fiber Metal Laminated Plates - Experimental and Numerical Studies. *International Journal of Structural Stability and Dynamics*. 18(11), 1850144.
- [21] E.V. Prasad, Chinnam Sivateja and S.K. Sahu, 2020. Effect of nanoalumina on fatigue characteristics of fiber metal laminates, *Polymer Testing, Volume 85*, 106441, ISSN 0142-9418,
- [22] Pruthwiraj Sahu, Nitin Sharma and Subrata Kumar Panda, 2020. Numerical prediction and experimental validation of free vibration responses of hybrid composite (Glass/Carbon/Kevlar) curved panel structure, *Composite Structures, Volume 241*, 112073, ISSN 0263-8223.
- [23] Sahu, P., Sharma, N., Dewangan, H.C. and Panda, S.K., 2022. Theoretical Prediction and Experimental Validity of Thermal Frequency Responses of Laminated Advanced Fiber-Reinforced Epoxy Hybrid Composite Panel. *International Journal of Structural Stability and Dynamics*, 22(8), 2250088.
- [24] Sahu, P., Sharma, N., Dewangan, H. C., and Panda, S. K. 2022. Thermo-Mechanical Transient Flexure of Glass-Carbon-Kevlar-Reinforced Hybrid Curved Composite Shell Panels: An Experimental Verification, *International Journal of Applied Mechanics*, vol. 14(1).
- [25] Kulmani Mehar, Subrata Kumar Panda, and Nitin Sharma, 2020. Numerical investigation and experimental verification of thermal frequency of carbon nanotube-reinforced sandwich structure, *Engineering Structures, Volume 211*, 110444, ISSN 0141-0296.
- [26] Mehar, K.; Mishra, P. K. and Panda, S. K. 2020. Numerical investigation of thermal frequency responses of graded hybrid smart nanocomposite (CNT-SMA-Epoxy) structure. *Mechanics of Advanced Materials and Structures*, pp.1-13.
- [27] Sahoo, S. S., Hirwani, C. K., Panda, S. K. and Sen, D. 2018. Numerical analysis of vibration and transient behaviour of laminated composite curved shallow shell structure: An experimental validation, *Scientia Iranica*, 25(4), pp. 2218-2232.
- [28] Sharma, Narayan., Swain, Prasant Kumar., Maiti, D. K. and Singh, B. N. 2020. Stochastic frequency analysis of laminated composite plate with curvilinear fiber. *Mechanics of Advanced Materials and Structures*, pp.1-16.
- [29] Sharma, N., Nishad, M., Maiti, D. K., Sunny, M. R., and Singh, B. N. 2021. Uncertainty quantification in buckling strength of variable stiffness laminated composite plate under thermal loading. *Composite Structures*, 275, 114486.
- [30] Sharma, N., Swain, P. K., Maiti, D. K., and Singh, B. N. 2021. Stochastic aeroelastic analysis of laminated composite plate with variable fiber spacing. *Journal of Composite Materials*, 55(30), pp.4527-4547.
- [31] Sharma, N., Swain, P. K., Maiti, D. K., and Singh, B. N. 2022. Static and free vibration analyses and dynamic control of smart variable stiffness laminated composite plate with delamination. *Composite Structures*, 280, 114793.
- [32] Sharma, N., Swain, P. K., and Maiti, D. K. 2022. Aeroelastic control of delaminated variable angle tow laminated composite plate using piezoelectric patches. *Journal of Composite Materials*, 56(29), pp.4375-4408.
- [33] Sharma, N., Swain, P. K., and Maiti, D. K. 2022. Active flutter suppression of damaged variable stiffness laminated composite rectangular plate with piezoelectric patches. *Mechanics of Advanced Materials and Structures*, pp.1-21.
- [34] Swain, P. K., Sharma, N., Maiti, D. K., and Singh, B. N. 2020. Aeroelastic analysis of laminated composite plate with material uncertainty. *Journal of Aerospace Engineering*, 33(1).
- [35] Sharma, N., Tiwari, P., Maiti, D. K., and Maity, D. 2021. Free vibration analysis of functionally graded porous plate using 3-D degenerated shell element. *Composites Part C: Open Access*, 6, 100208.
- [36] Sharma, N., Kumar Swain, P., Kumar Maiti, D., and Nath Singh, B. 2022. Vibration and Uncertainty Analysis of Functionally Graded Sandwich Plate Using Layerwise Theory. *AIAA Journal*, 60(6), pp.3402-3423.